Supporting Information for:
Nonadiabatic dynamics simulations of photoexcited urocanic acid

Deniz Tuna[1*], Lasse Spörkel[1], Mario Barbatti[2], and Walter Thiel[1]

[1] *Max-Planck-Institut für Kohlenforschung, 45470 Mülheim an der Ruhr, Germany*

[2] *Aix Marseille Univ, CNRS, ICR, Marseille, France*

[*] *email: tuna@kofo.mpg.de*

Comments on the choice of the active orbitals

The (12,10) active space used by us comprises all important π and π^* MOs of urocanic acid (see Fig. S1). Only the two lowest-lying π MOs are excluded because they are so low in energy that they practically do not participate in the low-lying excited states. Several of the π and π^* MOs included in our active space have a stronger weight on the imidazole ring, therefore ring-puckering processes and changes in the local basicity of this ring are describable by this active space. Other π or π^* MOs have a stronger weight on the acid moiety, therefore changes in the acidity of the acid moiety can also be captured by this active space. Changes in the acidity or basicity of these two moieties are driven by shifts in electron density through charge-transfer $\pi\pi^*$ or $n\pi^*$ transitions. Such transitions induce ESIPT processes, which are electron-driven proton-transfer processes.

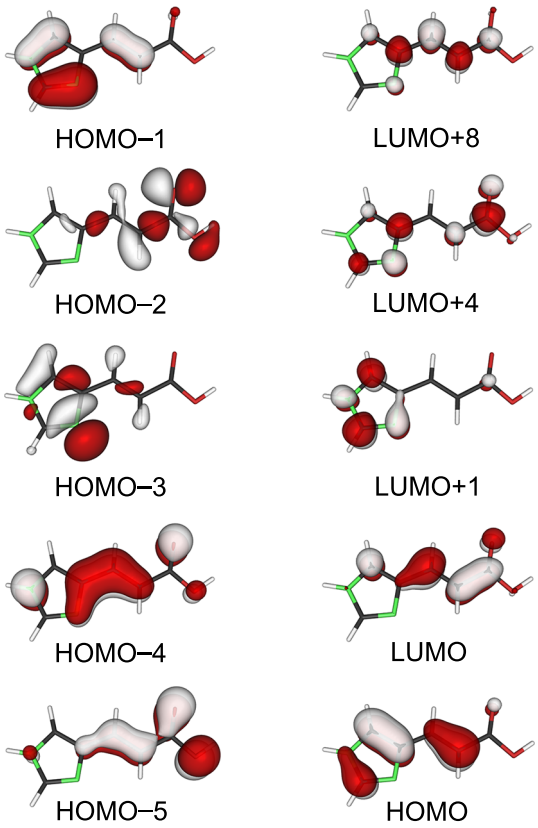

Figure S1 Molecular orbitals in the (12,10) active space of the N3H-*tEct* isomer. The HOMO−3 is the n_N lone-pair MO, the HOMO−2 is the n_O lone-pair MO.

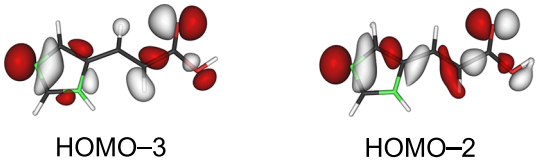

Figure S2 Lone-pair MOs in the active space of the N1H-*tEct* isomer.

Table S1 Vertical excitation energies (in eV) and oscillator strengths (in parentheses) of the lowest five singlet excited valence states of eight E and Z isomers of the N1H and N3H tautomers of UA. OM2/MRCI results are compared with previous MS-CASPT2 and CC2 results.[2] Red color denotes $n\pi^*$ states, blue color denotes $\pi\pi^*$ states. Details are given in the Computational Methods section in the article.

	OM2/MRCI				
isomer	S_1	S_2	S_3	S_4	S_5
N3H-*tEct*	4.94 (0.5345)	4.98 (0.0010)	5.31 (0.1331)	6.15 (0.0017)	6.26 (0.2534)
N3H-*tEtc*	4.76 (0.0010)	4.98 (0.4798)	5.35 (0.2220)	6.11 (0.0018)	6.31 (0.1953)
N1H-*tEct*	4.59 (0.6599)	4.86 (0.0010)	5.42 (0.0049)	5.65 (0.0639)	5.76 (0.0006)
N1H-*tEtt*	4.59 (0.6853)	4.87 (0.0011)	5.42 (0.0058)	5.64 (0.0659)	5.77 (0.0006)
N3H-*tZct*	4.79 (0.0015)	4.88 (0.4465)	5.30 (0.1499)	5.82 (0.0018)	6.17 (0.0071)
N3H-*tZtc*	4.60 (0.0014)	5.12 (0.3223)	5.35 (0.3635)	6.29 (0.1209)	6.50 (0.1108)
N1H-*tZct*	4.19 (0.4924)	5.01 (0.0016)	5.25 (0.0013)	5.52 (0.0001)	5.52 (0.0506)
N1H-*tZtt*	4.37 (0.6037)	4.99 (0.0014)	5.33 (0.0024)	5.54 (0.0959)	5.62 (0.0002)
	MS-CASPT2				
isomer	S_1	S_2	S_3	S_4	S_5
N3H-*tEct*	4.83 (0.3526)	5.14 (0.0006)	6.06 (0.0639)	6.47 (0.0012)	6.95 (0.0174)
N3H-*tEtc*	4.75 (0.0006)	4.99 (0.6985)	6.25 (0.0681)	6.42 (0.0010)	6.93 (0.0175)
N1H-*tEct*	4.39 (0.3761)	5.09 (0.0005)	6.09 (0.0044)	6.21 (0.1207)	6.45 (0.2532)
N1H-*tEtt*	4.48 (0.4928)	5.02 (0.0006)	6.10 (0.0045)	6.25 (0.1391)	6.47 (0.1779)
N3H-*tZct*	4.72 (0.0011)	4.78 (0.2858)	6.09 (0.0009)	6.10 (0.0606)	6.61 (0.0162)
N3H-*tZtc*	4.50 (0.0004)	5.75 (0.1401)	6.84 (0.0463)	7.02 (0.0133)	7.14 (0.0122)
N1H-*tZct*	4.05 (0.2798)	5.20 (0.0004)	5.72 (0.0013)	6.16 (0.1371)	6.26 (0.1702)
N1H-*tZtt*	4.31 (0.4416)	5.07 (0.0006)	5.92 (0.0024)	6.22 (0.1043)	6.37 (0.2589)
	CC2				
isomer	S_1	S_2	S_3	S_4	S_5
N3H-*tEct*	5.05 (0.0001)	5.18 (0.6547)	6.22 (0.0938)	6.24 (0.0010)	6.83 (0.1360)
N3H-*tEtc*	4.69 (0.0002)	5.25 (0.6130)	6.22 (0.0011)	6.27 (0.1236)	6.87 (0.0919)
N1H-*tEct*	4.80 (0.7309)	5.02 (0.0001)	5.64 (0.0001)	6.03 (0.0066)	6.78 (0.0008)
N1H-*tEtt*	4.83 (0.7504)	4.95 (0.0001)	5.66 (0.0001)	6.03 (0.0051)	6.81 (0.0008)
N3H-*tZct*	4.63 (0.0002)	5.16 (0.5578)	5.89 (0.0008)	6.24 (0.1051)	6.68 (0.0050)
N3H-*tZtc*	4.39 (0.0001)	5.51 (0.5244)	6.21 (0.1582)	6.37 (0.0335)	6.46 (0.0001)
N1H-*tZct*	4.39 (0.5209)	5.05 (0.0000)	5.41 (0.0000)	5.66 (0.0062)	6.78 (0.0368)
N1H-*tZtt*	4.62 (0.6221)	5.04 (0.0001)	5.46 (0.0000)	5.86 (0.0054)	6.85 (0.0888)

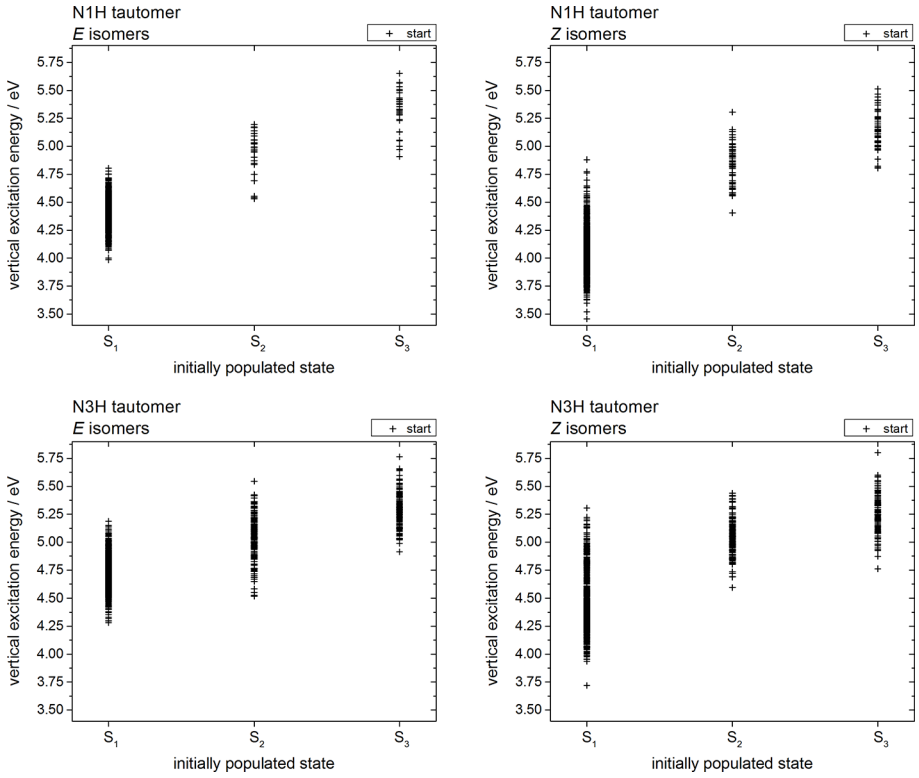

Figure S3 Vertical excitation energies of the three lowest singlet excited states at the beginning of each trajectory and distribution of initially populated states of the initial conditions for the TSH dynamics simulations. The analysis is presented for each of the four classes of isomers and tautomers.

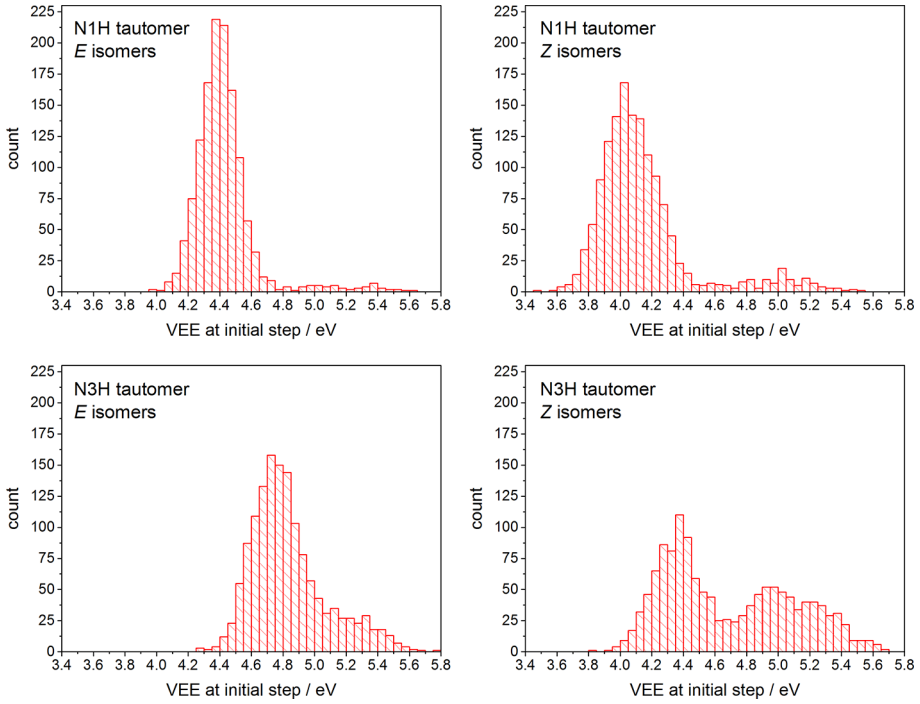

Figure S4 Histograms of the vertical excitation energies of the initially populated state at the starting geometry of each trajectory. This analysis is presented for each of the four classes of isomers and tautomers.

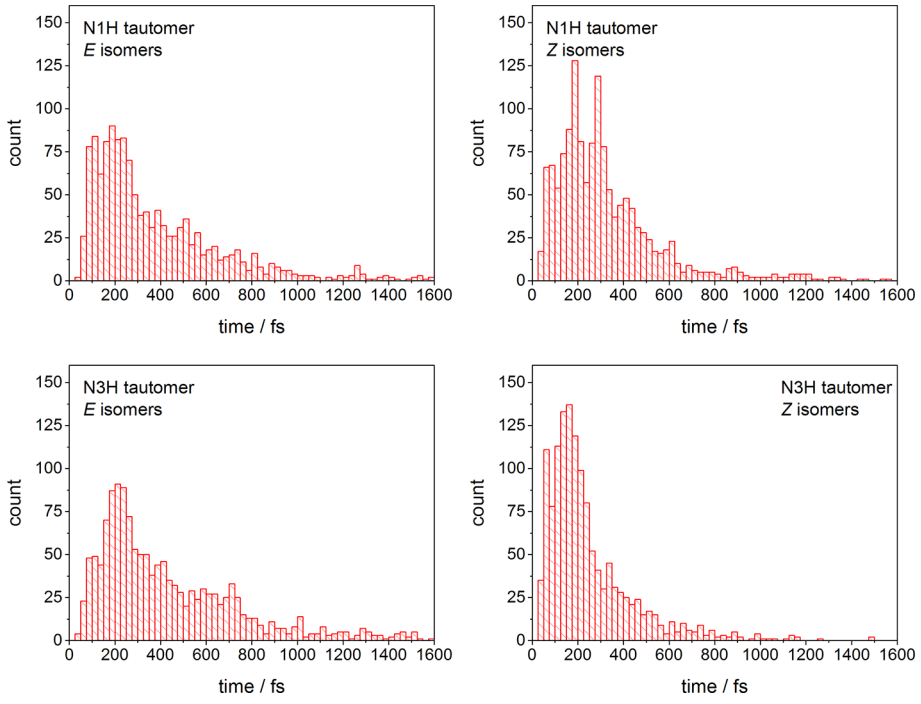

Figure S5 Histograms of the S_1/S_0 hopping times. This analysis is presented for each of the four classes of isomers and tautomers.

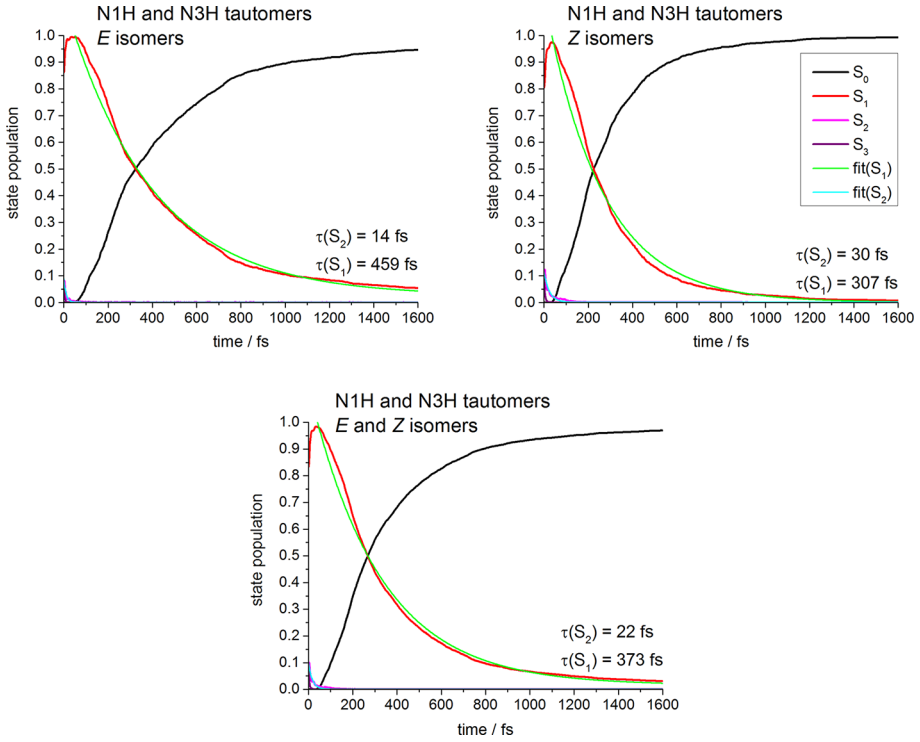

Figure S6 Average state populations of S_0–S_3 (black, red, magenta, purple) for the ensembles of all *E* isomers and all *Z* isomers, respectively, of both tautomers (top) and of all isomers of both tautomers (bottom). The depletions of the S_2 and S_1 state populations were fitted with a monoexponential decay function (cyan and green). The computed excited-state lifetimes of S_2 and S_1 (given as the sum of the initial delay time and the fitted decay time) are printed in the lower right corner of each plot.

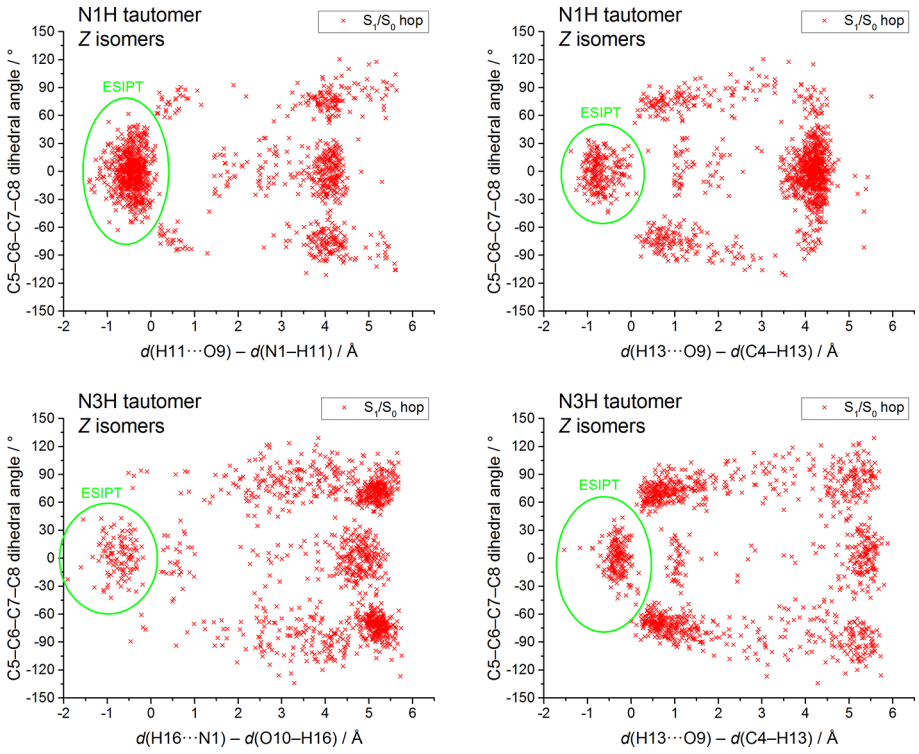

Figure S7 S_1/S_0 hopping points in the two-dimensional coordinate space of the central C5−C6−C7−C8 dihedral angle and the ESIPT coordinate. The latter is expressed as the difference in internuclear distances of each atom triple involved in the two possible ESIPT processes of the *Z* isomers of each of the two tautomers. The two defining internuclear distances *d* (see label on *x* axes) are indicated by double-ended arrows on the structural formulas shown in Fig. 11 in the paper. A negative difference of the internuclear distances at the S_1/S_0 hopping point indicates that the S_1/S_0 deactivation process involves an ESIPT. ESIPT events are marked by a green ellipse.

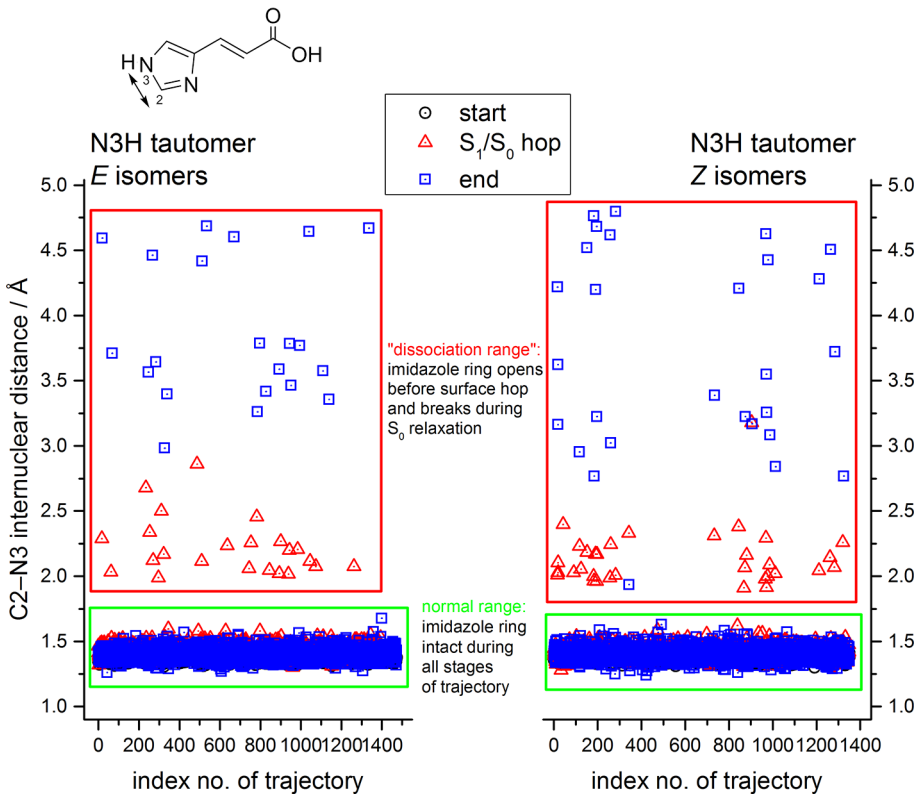

Figure S8 Ring-opening side reaction of the imidazole moiety in the *E* and *Z* isomers of the N3H tautomer. The plots show the C2–N3 internuclear distance on the y axis (the x axis is a counter). Shown for each trajectory: starting geometry (black circles); S_1/S_0 hopping point (red triangles); final geometry (blue rectangles). In the normal range (green rectangles) the three critical points of the trajectories are all clustered around a C2–N3 distance of 1.5 Å, where the imidazole ring is intact. In the dissociation range (red rectangles) the C2–N3 distance is elongated at the S_1/S_0 hopping point, which suggests a ring-opening pathway. In some geometries, the ring has broken at the final geometry (blue squares in the top part of the red rectangle).

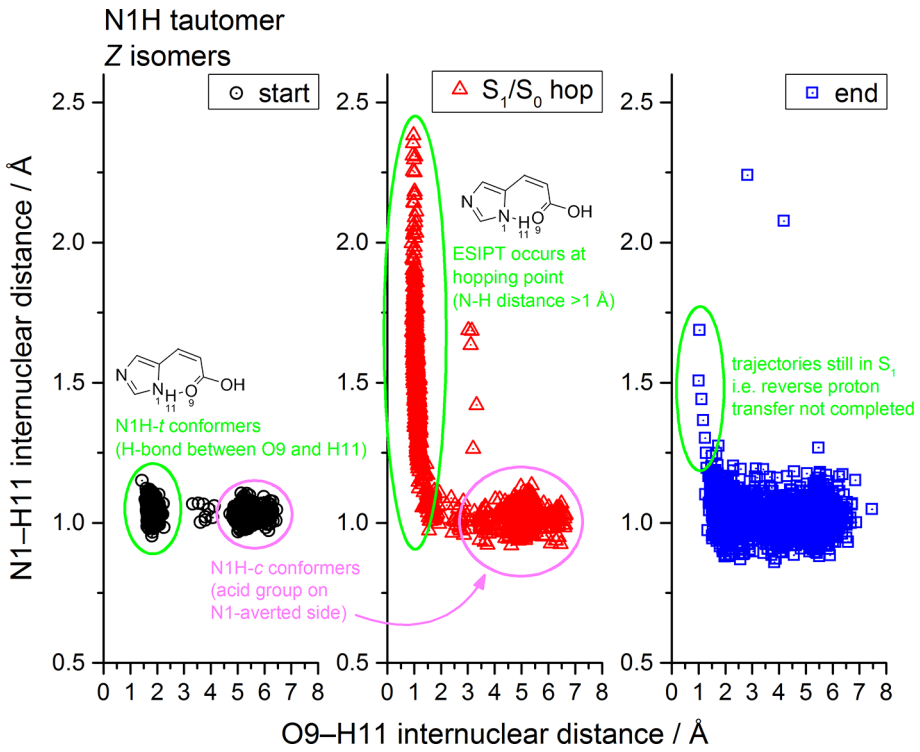

Figure S9 ESIPT process in the N1H-*tZ* conformers, in which the proton is transferred from the NH group of the imidazole moiety to the oxygen atom of the acid moiety. The three plots show the distribution of the O9–H11 and N1–H11 internuclear distances in the trajectories of the *Z* isomers of the N1H tautomer: left, starting geometry (black circles); middle, S_1/S_0 hopping point (red triangles); right, final geometry (blue rectangles). The N1H-*tZ* conformers and ESIPT-related structures are marked by green ellipses. There are six trajectories where the proton remains on the acid moiety at the end (green ellipse, right). These trajectories are still in the excited state at the end of the simulation time.

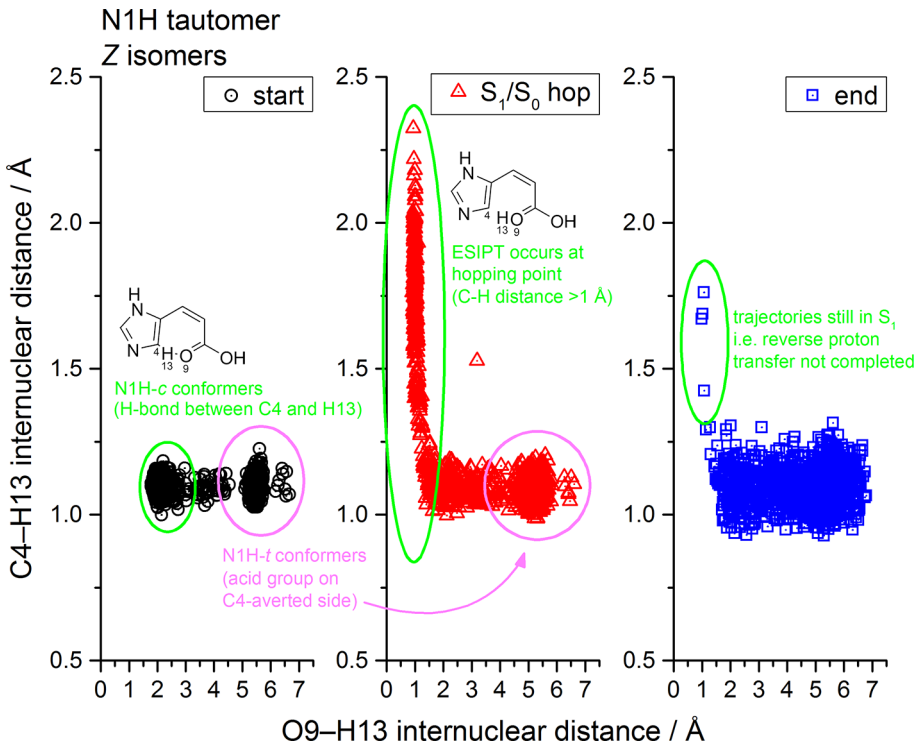

Figure S10 ESIPT process in the N1H-cZ conformers, in which the proton is transferred from the CH group of the imidazole moiety to the oxygen atom of the acid moiety. The three plots show the distribution of the O9–H13 and C4–H13 internuclear distances in the trajectories of the Z isomers of the N1H tautomer: left, starting geometry (black circles); middle, S_1/S_0 hopping point (red triangles); right, final geometry (blue rectangles). The N1H-cZ conformers and ESIPT-related structures are marked by green ellipses. There are four trajectories where the proton remains on the acid moiety at the end (green ellipse, right). These trajectories are still in the excited state at the end of the simulation time.

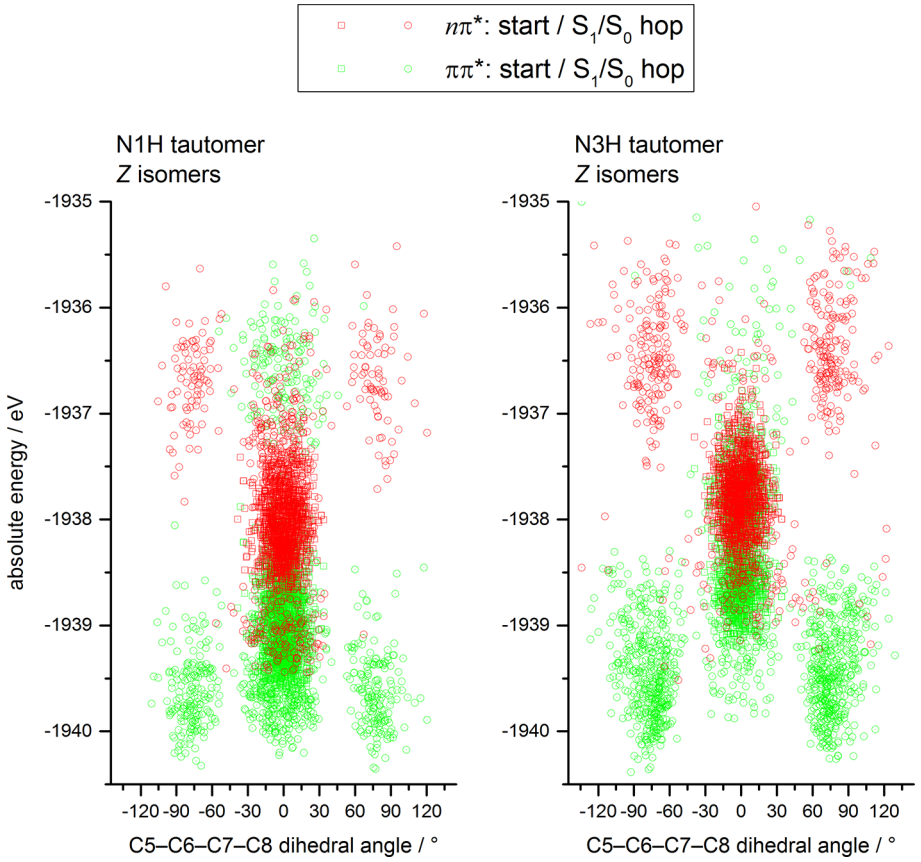

Figure S11 Absolute energies (in eV) of the $n\pi^*$ (red) and $\pi\pi^*$ (green) states at the starting geometries (squares) and S_1/S_0 hopping points (circles) of each trajectory of the Z isomers of the N1H and N3H tautomers. The x axis shows the value of the central dihedral angle.

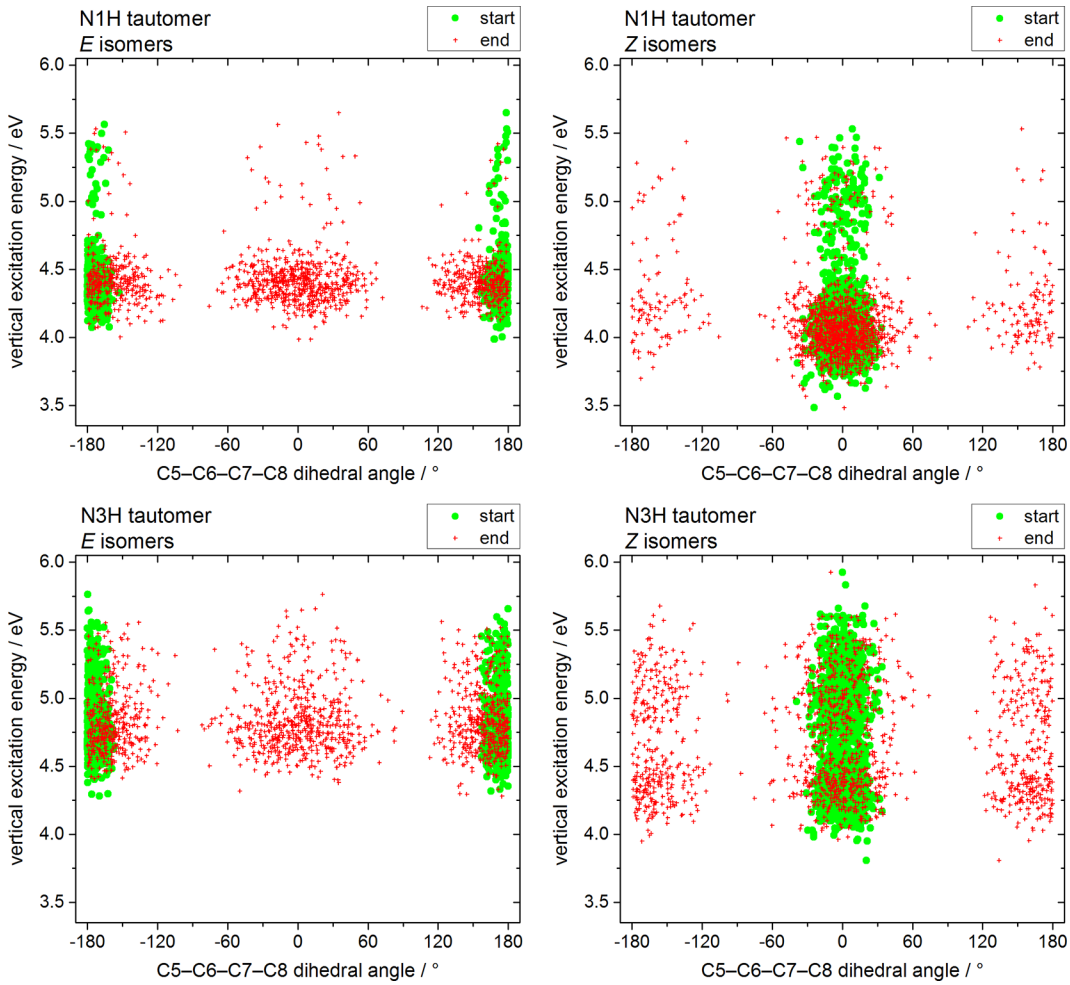

Figure S12 Central dihedral angle at the starting geometry (green dots) and the final geometry (red crosses) of each trajectory plotted against the vertical excitation energy of the optically excitable initially populated state at the beginning of each trajectory. Green dots and red crosses that belong to the same trajectory are found on an imaginary horizontal line. This analysis is presented for each of the four classes of isomers and tautomers.

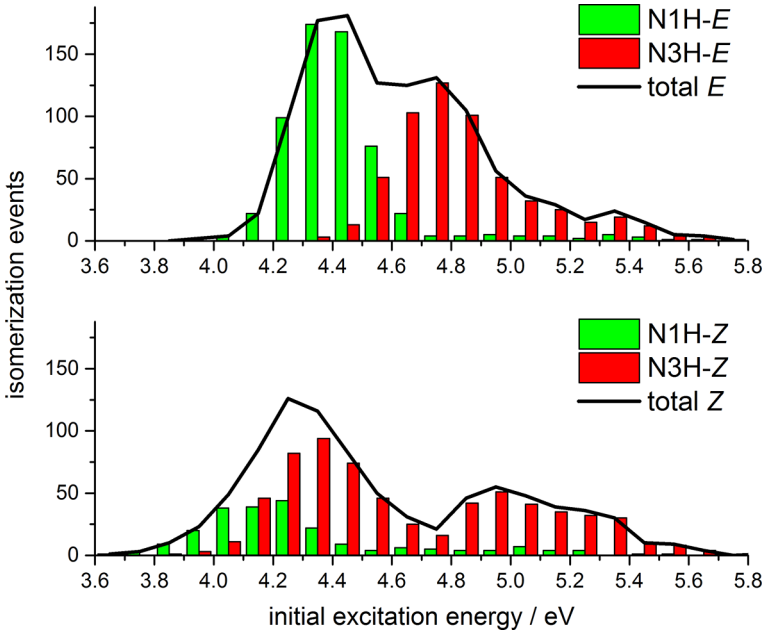

Figure S13 Histograms of isomerization events as a function of the initial excitation energy for the E and Z isomers of the N1H and N3H tautomers.

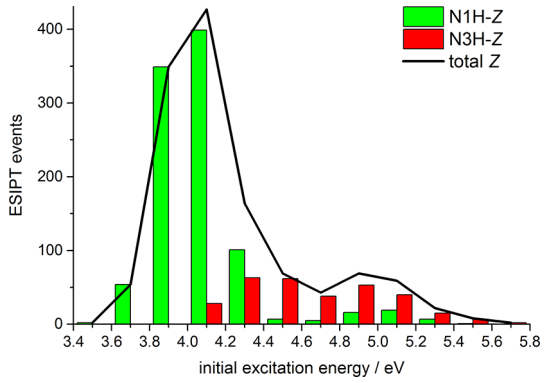

Figure S14 Histograms of ESIPT events as a function of the initial excitation energy for the Z isomers of the N1H and N3H tautomers.

Details on the performance of OM2/SCF and SCC-DFTB on the relative stability of conformers

We decided against using the OM2/SCF method for the ground-state MD simulations, because it failed to reproduce the relative stability of two crucial conformers of UA. One of us (Barbatti) has presented in a previous study[1] that the two conformers N3H-*tZtc* and N3H-*cZct* (see Fig. 2 in the article) are 0.90 kcal/mol apart in energy at the DFT(B3LYP)/TZVP level of theory. The more stable of these two conformers is the N3H-*cZct* conformer. The slightly less stable N3H-*tZtc* conformer exhibits an intramolecular hydrogen bond between the OH group of the acid moiety and the N1 atom of the imidazole moiety. In a previous study led by one of us (Tuna) it was shown that this conformer can be expected to deactivate via an intramolecular excited-state proton transfer.[2] Unfortunately, at the OM2/SCF (OM2/MRCI) level, the N3H-*cZct* conformer is 7.01 (5.52) kcal/mol more stable than the N3H-*tZtc* conformer, effectively removing the N3H-*tZtc* conformer from the sample of initial structures. Using OM2/SCF (OM2/MRCI) with D3 dispersion correction lowers the energy difference slightly to 6.81 (5.37) kcal/mol, which gives a slight improvement, but still heavily overestimates the relative stability of the N3H-*cZct* conformer over the N3H-*tZtc* conformer. At the SCC-DFTB level, the energy difference goes down to 4.52 kcal/mol, which is still not perfect compared to the value of 0.90 kcal/mol at the DFT level, but this at least leads to some contribution of the N3H-*tZtc* conformer in the sample of initial structures. For this reason, we have decided to use the SCC-DFTB method for all ground-state MD simulations of the 32 conformers of UA. In summary, this shows that the OM2/SCF method may have some deficiencies in describing the relative ground-state stability of the many different conformers of UA (for a subset of these see the paper by Barbatti[1]), especially in conformers involving hydrogen bonds.

References

[1] M. Barbatti, *Phys. Chem. Chem. Phys.* **2011**, *13*, 4686−4692.

[2] D. Tuna, A. L. Sobolewski, W. Domcke, *J. Phys. Chem. B* **2014**, *118*, 976−985.